ACS APPLIED MATERIALS & INTERFACES

Research Article

www.acsami.org

High Porosity Supermacroporous Polystyrene Materials with Excellent Oil–Water Separation and Gas Permeability Properties

Shuzhen Yu, Hongyi Tan, Jin Wang, Xin Liu, and Kebin Zhou*

School of Chemistry and Chemical Engineering, University of Chinese Academy of Sciences, Beijing 100049, People's Republic of China

Supporting Information

ABSTRACT: Two types of monolith high-porosity supermacroporous polystyrene materials had been controlled synthesized from water-in-oil Pickering emulsions. The first type, closed-cell high-porosity (up to 91%) supermacroporous (ca. 500 μm) polystyrene materials (CPPs) was prepared by employing amphiphilic carbonaceous microspheres (CMs) as high internal phase emulsion stabilizer without any inorganic salts or further modifying the wettability of the particles. The second type, hierarchical porous polystyrene materials with highly interconnected macropores (IPPs), was constructed from emulsions stabilized simultaneously by CM particles and a little amount of surfactants. Both types of these monolith porous polystyrene materials possessed excellent mechanical strength. The CPPs were used as absorbents for oil–water separation and high absorption capacity, and absorption rate for oils were realized, which was attributed to their porosity structure and the swelling property of the polystyrene, while the IPPs were highly permeable for gases due to their interconnected macropores.

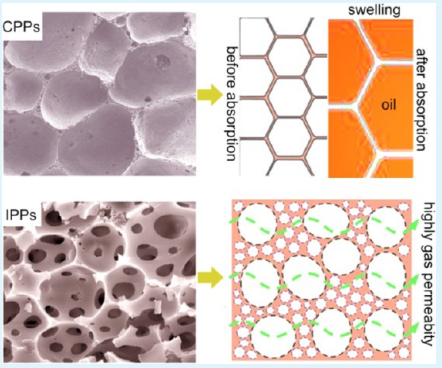

KEYWORDS: *high porosity, supermacroporous, polystyrene, oil–water separation, gas permeability*

INTRODUCTION

Porous polymers have been the subject of intense interest due to their wide applications, such as gas storage and separation,[1−4] tissue engineering,[5,6] supports for catalyst,[7−10] and many others.[11−13] For satisfying these applications, it is of great importance to prepare supermacroporous polymeric monolith materials with high porosity, tunable interconnection of pores, and desired mechanical properties.

Until now, several synthesis methods, like direct templating,[14] block copolymer self-assembly,[15,16] and interfacial polymerization,[17] have been developed to obtain special structure and framework of porous polymers. Among various strategies, high internal phase emulsion (HIPE) polymerization has been considered as one of the most efficient methods for preparing highly porous and permeable polymeric materials with well-defined porosity and low foam density.[18,19] HIPEs are concentrated emulsion systems possessing a volume of internal phase more than 74%, meanwhile the spherical droplets of dispersed phase are deformed into polyhedra and separated by thin films of continuous phase.[20−22] When monomers are used as the continuous phase of water-in-oil HIPEs, polymerized high internal phase emulsion (poly-HIPEs) with high porosity will be fabricated via polymerization of the monomers. However, preparation of conventional poly-HIPEs requires a large quantity of surfactants, and thus has high costs, and usually results in porous materials with poor mechanical properties[23,24] which limits their practical applications.

Recently, particles rather than surfactants stabilized Pickering HIPEs have received considerable attentions since Vivian et al.[20] first reported that up to 92% internal phase Pickering emulsions could be stabilized with SiO_2 particles and further polymerized into high porosity polystyrene materials. Compared with conventional poly-HIPEs, poly-Pickering-HIPEs prepared from particles stabilized water-in-oil HIPEs show significant advantages in lower cost and elimination of the postremoval of surfactants.[19,25] However, only limited categories of particles have been developed for stabilizing water-in-oil poly-HIPEs due to the demand of special amphiphilicity. For example, hydrophobic carbon nanotubes could be used as stabilizer for poly-HIPEs only after functionalization of an amphiphilic block copolymer. On the other hand, inorganic particles such as titania,[21] silica[20,26] and magnetic nanoparticles[27] are too hydrophilic to stabilize HIPEs. And modifying with hydrophobic molecules (such as oleic acid) is necessitated to adjust their wettability. Moreover, addition of salts such as $CaCl_2$ is commonly needed to further promote emulsion stability via lowering the electrostatic barriers of particles adsorption at the oil–water interfaces.[21,28] There is still an urgent call for exploring low-cost, versatile particles and simple methods for the preparation of poly-Pickering-HIPEs.

In our previous studies,[29,30] amphiphilic hollow carbonaceous microspheres (CMs) were synthesized via mild hydrothermal treatment of yeast cells. The wettability of CMs could be facilely tuned by adjusting the hydrothermal treatment

Received: January 8, 2015
Accepted: March 11, 2015
Published: March 11, 2015

DOI: 10.1021/acsami.5b00196
ACS Appl. Mater. Interfaces 2015, 7, 6745−6753

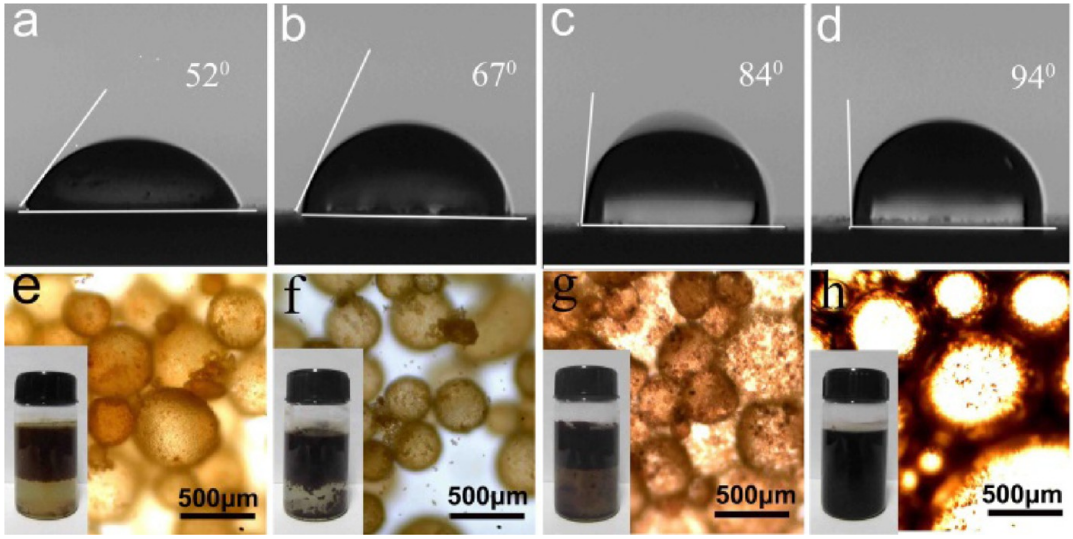

Figure 1. Air–water contact angles for (a) CM170, (b) CM180, (c) CM190, and (d) CM210. (e–h) Corresponding optical microscopy images of the Pickering emulsions formed with a water–styrene/DVB ratio of 74:26 stabilized by CM 170–210, respectively; (insets) photos of the Pickering emulsions.

temperature during synthesis and Pickering emulsions could be formed when these amphiphilic CMs were dispersed in water–oil biphasic media.[31,32] Employing carbonaceous microspheres as stabilizer, we report herein that high internal phase water-in-oil emulsions can be facilely assembled without any inorganic salts or tedious modifying the wettability of the particles. After polymerization of the continuous styrene monomer phase, closed-cell high porosity supermacroporous polystyrene materials (CPPs) have been successfully prepared. Moreover, hierarchical porous polystyrene materials with highly interconnected macropores (IPPs) have also been created from emulsions stabilized simultaneously by CM particles and a small amount of surfactants. Most importantly, these monolith porous materials exhibited good mechanical strength, excellent oil–water separation and gas permeability properties.

EXPERIMENTAL SECTION

Materials. All the reagents were purchased from commercial sources (Sinopharm, Xiya, Tianjin Guangfu, or Beijing Chemical Co.). Active dry yeast was supplied by Angel Yeast Co., Ltd. CMs were synthesized via the hydrothermal treatment of yeast cells using the methods described in our previous work.[19,29]

Synthesis of Porous Polystyrene Materials. Prior to emulsification, inhibitors were removed from monomers styrene and divinylbenzene (DVB). Then, 14 wt % (with respect to monomer) of CMs was first dispersed in the monomers (mixture of styrene and DVB in various ratios) under ultrasonication. Next, 1 mol % of 2,2′-azobis(2,4-dimethylvaleronitrile) (V-65) initiator (with respect to the monomers) was added to this mixture. The proper amount of inner water phase was dropped gradually to the suspension. Afterward, the suspension was put in an ultratube disperser (IKA ultra turrax) and stirred fiercely at 1000 rpm for 1 min to form the Pickering emulsions. Finally the Pickering emulsions were polymerized at 50 °C for 24 h. Then CPPs were obtained after drying. To prepare the IPPs, surfactant sorbitan monooleate (SPAN 80) (varying 2–7 vol % with respect to monomer), 14 wt % of CMs and 1 mol % of V-65 initiator were dissolved in mixture of styrene and DVB (1:1 volume). Then, the 74 vol % aqueous internal phase was added into the solution above under fiercely stirring at 1000 rpm for 1 min. The resulted emulsions were polymerized at 50 °C for 24 h. And the IPPs could be obtained after drying.

Oil–Water Separation and Gas Permeability. Oil–water separation properties of the materials were investigated for the various organic solvents and oils. First, the porous materials were cut into a 1 × 1 × 1 cm cubic sample. Then, the sample was put into the oil–water mixtures and was collected after absorption for weight and volume measurements. The mass absorption capacity (M_{abs}), volume absorption capacity (V_{abs}), and swell ratio were determined by the following equation:

$$M_{abs} = (M_{sat} - M_0)/M_0$$

$$V_{abs} = (M_{sat} - M_0)/\rho V_0$$

$$\text{swell ratio} = V_{sat}/V_0$$

where M_{sat} and M_0 indicate the mass of the porous material before (0) and after (sat) saturation by organic solvents or oil, respectively, and V_{sat} and V_0 are the volumes of the porous material accordingly. The absorbing selectivity was calculated by the ratio (S (%)) between the absorbed oil and absorption quantity after treatment, according to the following equation:

$$S(\%) = (M_i - M_r)/(M_{sat} - M_0)$$

where M_i and M_r are the oil weight of the initial oil/water mixture and the residual oil after treatment. M_r could be obtained by the residual oil that was extracted from treated mixture and analyzed the UV–vis spectrometer (Shimadzu UV2550).[33] Gas permeability was carried out with a home-built sample cell using the pressure rise technique.[34] The viscous permeability was obtained according to Darcy's law.

Characterization. Morphology of CMs and the porous polymeric materials were measured by scanning electron microscopy (SEM, Hitachi S-4800). Fourier transform infrared spectroscopy was made by a Bruker VERTEX 70. The contact angles were investigated by a contact angle measuring instrument (JC2000C1). Porosities of the materials were calculated after measuring skeleton density (ρs) and foam density (ρf). The mechanical tests of the porous polymeric materials were measured by material testing machine (Hengyi HY-0580) according to BS ISO 844.

RESULTS AND DISCUSSION

Preparation of CPPs. CMs were synthesized via mild hydrothermal treatment of yeast cells at 170, 180, 190, and 210 °C and denoted as CM170, CM180, CM190, and CM210, respectively (Figure S1, Supporting Information).[29,30] Air–

DOI: 10.1021/acsami.5b00196
ACS Appl. Mater. Interfaces 2015, 7, 6745–6753

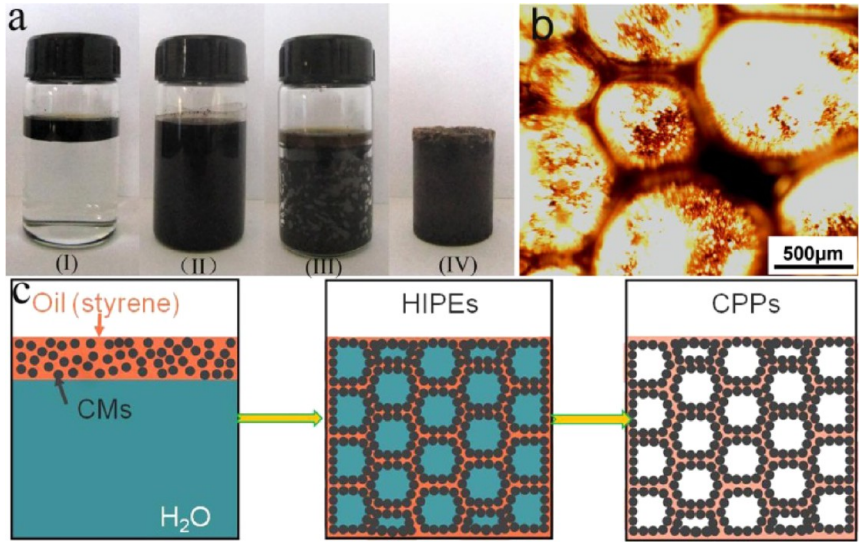

Figure 2. (a) Preparing process for poly-Pickering-HIPEs: (I) biphase water−styrene/DVB that contained CMs before HIPEs formation, (II) W/O HIPEs stabilized by CMs, (III) after polymerization, (IV) obtained poly-Pickering-HIPEs. (b) Optical microscope image of HIPEs. (c) Schematic illustration of the formation strategy of the poly-Pickering-HIPEs.

water contact angles of the carbonaceous microspheres are shown in Figure 1a−d. It could be found that the hydrophobicity of CMs enhanced with increasing the synthesis temperature, which was caused by alternation the surface functional groups of CMs (Figure S2, Supporting Information).[29] For example, the contact angle of CM170 was 52°, showing a hydrophilic property, while CM210 exhibited amphiphilic characteristic with slight hydrophobicity. After stirring of the mixture of water, oil (styrene and divinylbenzene), and CMs, thick Pickering emulsion layers immediately formed. Due to the hydrophilic property of CM170−190, a phase inversion from water-in-oil (W/O) to oil-in-water (O/W) occurred before reaching 74% water to total volume (Figure 1e−g). However, CM210 could stay quite stable in W/O emulsions at 74:26 water−oil ratio due to their amphiphilicity (Figure 1h).[20] Because CM210 has appropriate wettability, we use it as the stabilizer in the rest of the studies to form Pickering HIPEs and further for porous polymer materials.

Through tuning the water to oil ratio synthesis factors, a series Pickering HIPEs with the internal phase volume from 74 to 85 vol % had been successfully prepared. The appearance of the Pickering HIPEs with an internal phase volume of 85 vol % after maintaining for 10 h is presented in Figure 2a(II), which indicates that the emulsions are highly stable against sedimentation. The corresponding optical microscopy image (Figure 2b) shows that deformed droplets with average diameter of 500 μm are formed and packed tightly together, and the polyhedral emulsions are separated by thin films of continuous oil phase. It should be noted that only pure water, oil (styrene and divinylbenzene), and CMs existed in the emulsion systems without any surfactant and inorganic salts, demonstrating the high efficiency of CMs to stabilize high internal phase emulsions (Figure S3, Supporting Information). As illustrated in Figure 2c, monolith polystyrene porous materials could be obtained after polymerizing the thin films of continuous oil phase of styrene monomers and subsequently removal of the internal phase water.

The porous materials were characterized by SEM and the results are shown in Figure 3 and Figure S4 (Supporting Information). For comparison, the SEM images of the poly-Pickering-emulsions with internal phase volume of 60% (denoted as CP0) are presented in Figure 3a,b. It could be

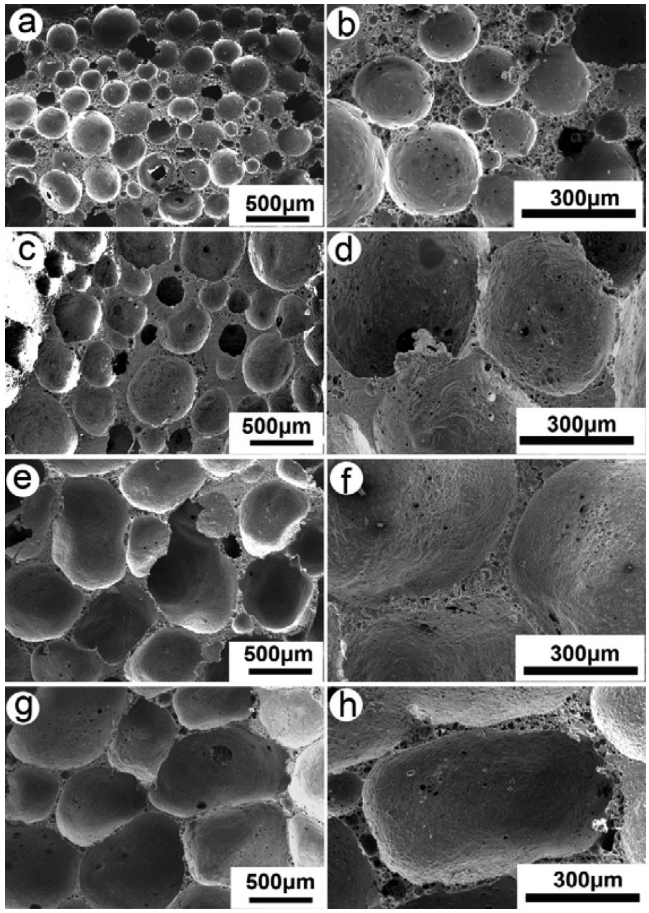

Figure 3. SEM images of porous materials synthesized from polymerization of water-in-oil Pickering emulsions with internal aqueous phase volume of (a and b) 60%, (c and d) 75%, (e and f) 80%, and (g and h) 85%.

DOI: 10.1021/acsami.5b00196
ACS Appl. Mater. Interfaces 2015, 7, 6745−6753

Table 1. Internal Phase Volume Ratio (Φ), Cross-Linker Concentration (Ψ) of Emulsion Template, Foam Density (ρf), Skeleton Density (ρs), Porosity (P), Crush Strength (σ), and Young's Modulus (E) of CPPs

sample	Φ (vol %)	Ψ (%)[a]	ρ_f (g/cm^3)	ρ_s (g/cm^3)	P (%)[b]	σ (MPa)	E (MPa)
CPPs0	60	1	0.266 ± 0.08	0.949 ± 0.002	72 ± 8	7.69 ± 1.9	103 ± 14
CPPs1	75	1	0.182 ± 0.03	0.904 ± 0.004	80 ± 3	6.05 ± 1.5	83 ± 17
CPPs2	80	1	0.147 ± 0.02	0.894 ± 0.004	84 ± 2	4.20 ± 1.2	75 ± 11
CPPs3	85	1	0.084 ± 0.04	0.882 ± 0.003	91 ± 3	4.43 ± 0.6	64 ± 7
CPPs4	85	2	0.098 ± 0.01	0.859 ± 0.007	89 ± 1	10.18 ± 0.1	191 ± 6
CPPs5	85	4	0.119 ± 0.02	0.676 ± 0.008	90 ± 2	10.30 ± 1.0	210 ± 18
CPPs6	85	10	0.125 ± 0.05	0.917 ± 0.009	87 ± 5	12.72 ± 0.9	291 ± 8

[a]Volume ratio of cross-linker (divinylbenzene) with respect to continuous phase. [b]Porosity calculated by foam density and skeleton density $P = 1 - \rho_f/\rho s$.

seen that spherical voids with average size about 210 μm had been inherited from the original Pickering emulsions, and most of the voids were separated by thick porous polystyrene wall. It should be noted that the poly-Pickering-HIPEs possessed mainly closed-cell voids, a typical structure of this kinds of materials. Figure 3c–h show the SEM images of the porous materials prepared from the emulsion templates with internal phase volume of 75, 80, and 85%, called CPPs1, CPPs2 and CPPs3, respectively. Once HIPEs were formed, the corresponding poly-Pickering-HIPEs exhibited nonspherical super void structures with void sizes of 200–700 μm. It was evident that the CPPs that originated from higher internal phase volume possessed larger average void size and wider size distribution. This phenomenon can be attributed to "limited coalescence" of emulsion droplets,[21,24,35,36] which occurs when comes to a large excess of oil–water interface with limited solid particles. Moreover, the compact degree of the voids were enhanced remarkably, and hence, polystyrene walls became thinner with increasing internal phase volume of emulsion template from 60 to 85%. The changes of the dense packing of voids result from a replica of the packing pattern of the emulsion templates, that is, the pore structure of CPPs can be facilely tailored by adjusting the water to oil ratio of the emulsion templates.

The porosities of the CPPs could be determined by measuring the skeleton densities (ρ_s) and foam densities (ρ_f) and the results are shown in Table 1. As expected, the skeleton densities were identical within the error because of the same constituents of the continuous phase of the emulsion templates, while the foam densities decreased with the increasing internal phase volume of the emulsion templates. The measured porosities of the CPPs were slightly higher than the internal phase volume of the corresponding emulsion templates (Table 1), owing to the sedimentation of emulsion template.[20] Despite the existence of sedimentation, it is still feasible to tune the porosities of CPPs by adjustable internal phase volume of emulsion template. As shown in Table 1, the porosities of CPPs are 72, 80, and 84% for the Pickering emulsion templates with internal phase volume of 60, 75, and 80%, respectively. Especially, up to 91% porosity of CPPs has been obtained by 85% internal phase HIPE template. This means that high porosity supermacroporous polystyrene materials have been constructed successfully.

Mechanical properties of porous material are a significant issue for practical applications. Therefore, the mechanical strength of the CPPs was measured, and the results are shown in Table 1. For all the CPPs, the values of crush strength and Young's modulus were higher than 4.2 and 64 MPa, respectively, revealing excellent mechanical properties when compared to many engineering foams, such as melamine, polystyrene, and even graphite foams.[37] Moreover, the mechanical strength of the CPPs can be further enhanced by increasing the amount of cross-linker (divinylbenzene, DVB) in the monomer phase of the emulsions before polymerization. For example, when 12 vol % DVB was employed, the values of crush strength and Young's modulus rose to 12.72 and 291 MPa, respectively. This can be attributed to the enhancement of the cross-linking density and thus reinforcement of the polymeric framework via increasing concentration of cross-linker.

Preparation of IPPs. For monolith porous materials, a high degree of interconnectivity of the pores is generally required to improve their permeability. As shown above, however, polymerization of Pickering-HIPEs generates mainly closed-cell porous polymeric materials. It had been reported that poly-Pickering HIPEs could transform closed-cell pores into interconnected pores by addition of surfactant as co-stabilizer.[23] Therefore, surfactant SPAN 80 was added into CMs stabilized Pickering emulsions to explore the possibility of formation of porous polystyrene materials with highly interconnected macropores. For comparison, the internal phase volumes were kept at 74% for all the starting emulsions. SEM images of the obtained materials are shown in Figure 4. Once 2 vol % SPAN 80 was added, it could be observed that both closed-cell supermacropores (>200 μm) and highly interconnected small pores (<20 μm) coexisted in the resulted materials (Figure 4a,b, denoted as IPPs1), that is, hierarchically structured porous polystyrene materials with highly interconnected macropores were constructed. The closed-cell supermacropores and the interconnected small pores are typical characteristics for poly-Pickering-HIPEs and conventional poly-HIPEs, respectively. This is attributed to the replica of the CMs and SPAN 80 co-stabilized emulsion template after polymerization,[38] which can be proved by distribution of CMs mainly on the walls of supermacropores (Figure S5, Supporting Information). By increasing the SPAN 80 content to 3 and 5 vol %, we can also obtain the same hierarchically interconnected pore structures for IPPs2 and IPPs3, as shown in Figure 4c–f. In addition, the size of the closed-cell supermacropores decreased and the number of pore throats per small pore increased. However, when the content of SPAN 80 increased to 7 vol %, the closed-cell supermacropores disappeared and were replaced completely by interconnected small pores (Figure 4g–h), as a result of surfactant SPAN 80 became the dominating emulsifier and the CMs are entirely excluded from the biphasic interfaces of the emulsions.[38] The physical properties such as the porosity and mechanical strength of the samples were also measured, and the results are summarized in Table 2. Synthesized from

DOI: 10.1021/acsami.5b00196
ACS Appl. Mater. Interfaces 2015, 7, 6745–6753

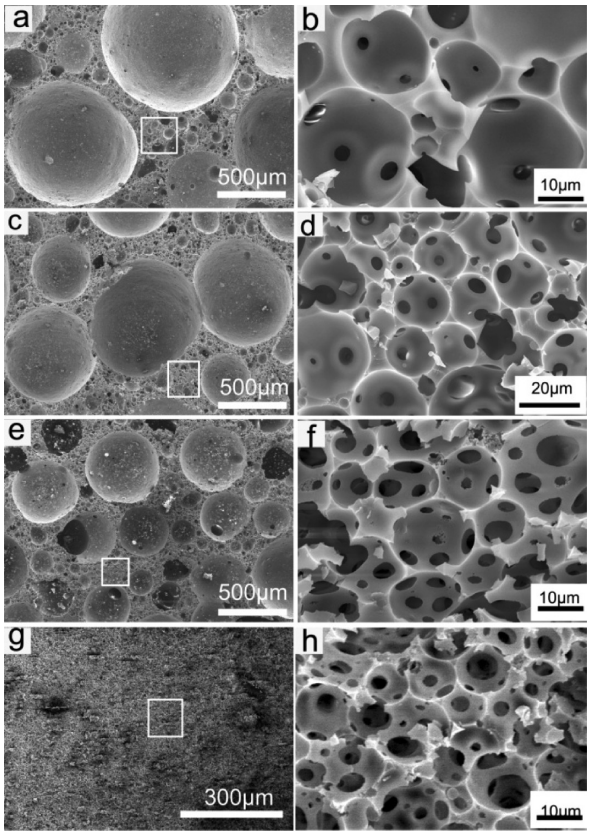

Figure 4. SEM images of hierarchical porous polystyrene materials with IPPs synthesized from polymerization of water-in-oil Pickering emulsions with adding various amounts of surfactant SPAN 80 (a and b) 2%, (c and d) 3%, (e and f) 5%, and (g and h) 7%. Panels b, d, f, and h are the high-magnification images of the regions marked with a box in panels a, c, e, and g, respectively.

emulsions with internal phase volume of 74%, the porosity of all the obtained porous materials fell in the range of 68−76%. The mechanical properties, crush strength and Young's modulus of the IPPs were still higher than that of the conventional poly-HIPE (the CPPs0 sample as shown in Table 2). It is well-known that introduction of particles into polymer matrix can usually increase their mechanical property, resulting from the interactions between particles and the polymer, which including electrostatic interactions,[39] interfacial bonding,[40] network bridging and so on.[41,42] Recently, Yang et al.[43] reported that the mechanical property of polyacrylonitrile (PAN) could be reinforced remarkably with the addition of CMs, which they proposed to act as cross-linking or network-bridging points to enhance the rigidity of the polymer chain. We suggest that similar interactions between CMs and polystyrene may exist in these porous polystyrene materials, leading to the promotion of mechanical properties of the IPPs.

Therefore, by employing amphiphilic carbonaceous microspheres as emulsion stabilizer, we have successfully synthesized CPPs. IPPs could also be constructed from emulsions stabilized simultaneously by CMs and surfactant SPAN 80. Both of these types of monolith porous materials possess high porosity, supermacropores and exhibit good mechanical strength, which make them versatile for practical applications.

Oil−Water Separation Performance of CPPs Oil Absorbents. Recently, organic solvent spills have drawn extensive attention due to economic and environmental concerns. The wettability of the as-obtained porous materials was investigated. As expected, all the materials exhibited hydrophobic and oleophilic characteristics. For example, the water contact angle of CPPs3 was 122° (Figure 5a), indicating that the sample was hydrophobic. When toluene was dropped on the surface of CPPs3, it could be immediately absorbed and caused slight swelling of the sample (Figure 5b), which demonstrates its oleophilic property. Because they repel water but absorb oil, these monolith porous materials were tested as oil absorption materials for the separation of oil and organic pollutants from water. Figure 5c shows the absorption capacities of the CPPs varying with the different porosity as an oil sorbent for toluene. It was found that the higher porosity of the material, the larger absorption capacity could be obtained. Possessing the highest porosity (91%), CPPs3 exhibited the highest absorption capacity (29.5 g/g) for toluene. In addition, the purity of collected toluene had also been investigated, and the result shows that with the porous CPPs3 materials, the oil ratio in the total collection is as high as 98.5%, indicating good selectivity of the materials for removing oils from water. The details of oil separation were further investigated over CPPs3 as a typical example, and Figure 5e and movie S1 (Supporting Information) present the whole process of cleaning toluene in water. When a piece of CPPs3 was placed on the surface of a toluene (dyed with red Sudan III) and water mixture. The toluene could be absorbed completely within 25 s, while the water was left. The absorption rate was measured, and the result is shown in Figure 5d. It was found that the absorption achieved saturation in 60 s, which is much faster than the conventional active carbon and nanoporous polymers (which reach absorbing saturation in 50 min or much longer).[44] It is important to note that a rapid swelling phenomenon of CPPs3 was observed along with the absorption of toluene from water, which enabled 3 times the volume absorption of toluene than its own volume (Figure 5f).

Table 2. Composition of Emulsion Template Characterized by Amount of Surfactant (Cs), Average Pore Size of Closed-Cell Super-Macropores (dp), Average Pore Size (ds) and Pore Throat (dt) of Highly Interconnected Small Pores, Porosity (P), Gas Permeability (κ), Crush Strength (σ), and Young's Modulus (E) of IPPs from Emulsions with 74% Internal Phase Volume

sample	Cs (vt %)[a]	dp (μm)	ds (μm)	dt (μm)	P (%)	k (D)[b]	σ (MPa)	E (MPa)
IPPs1	2	852 ± 31	15 ± 4	3.0 ± 1	74 ± 2	0.78 ± 0.14	2.00 ± 0.5	77 ± 10
IPPs2	3	622 ± 24	13 ± 3	3.5 ± 1	75 ± 3	1.35 ± 0.10	2.14 ± 0.2	72 ± 11
IPPs3	5	371 ± 18	9 ± 2	3.3 ± 1	68 ± 4	1.59 ± 0.19	3.26 ± 0.3	45 ± 10
IPPs4	7	0	8 ± 3	3.0 ± 1	76 ± 3	0.53 ± 0.18	3.16 ± 1.0	55 ± 6
CP0[c]	20	0	8 ± 1	2.4 ± 1	71 ± 1	0.40 ± 0.11	0.68 ± 0.7	11.93 ± 2
CPPs0	0	207 ± 9	0	0	72 ± 8	0.11 ± 0.08	7.69 ± 1.9	103 ± 14

[a]SP-80 with respect to continuous phase. [b]1 D = 10^{-12} m^2. [c]CP0 synthesized without adding any particles of CM210.

DOI: 10.1021/acsami.5b00196
ACS Appl. Mater. Interfaces 2015, 7, 6745−6753

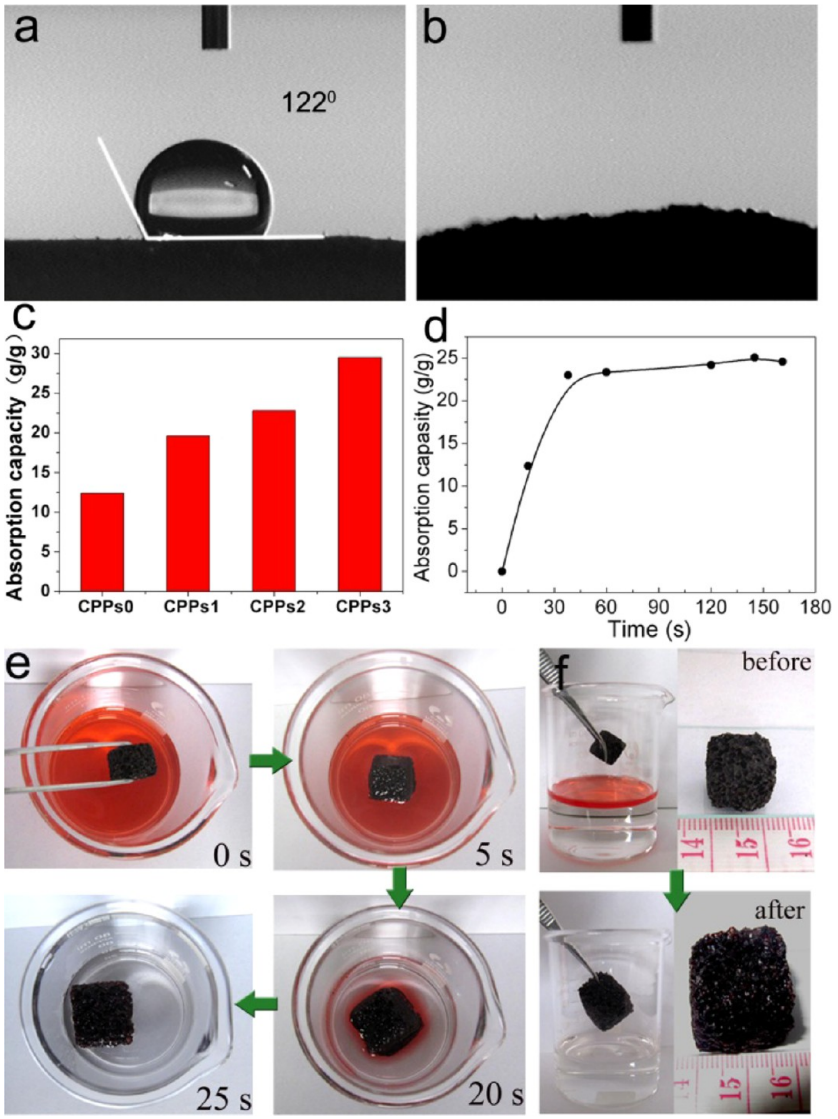

Figure 5. (a) Air−water and (b) air−toluene contact angles of CPPs3. (c) Absorption capacity of the as-prepared CPPs for toluene. (d) Absorption rate curve of CPPs3 for toluene. (e) Process of toluene absorption (dyed with Sudan III) from water within 25 s. (f) Photos of CPPs3 before and after toluene absorption.

The separation efficiency of CPPs3 for other organic solvents, such as decalin, tetrahydrofuran, chlorobenzene, and dichloromethane, had also been tested, and the results are summarized in Table 3. It could be seen that CPPs3 also exhibited high absorption capacity, which ranged from 470 to 3300 wt % for these organic liquids. The uptake efficiency was higher than that of other nanoporous polymer absorbents and commercial active carbon, such as polydimethylsiloxane sponge (400−1100 wt %),[45] nanoporous polydivinylbenzene (800−1500 wt %),[44] homocoupling polymerization of 1,4-diethynylbenzene (600−2300 wt %),[46] superhydrophobic polyurethane sponges (2100−3100 wt %),[47] superhydrophobic polyurethane sponge (1500−2500 wt %)[48] and active carbon (<100 wt %).[49] Interestingly, the porous CPPs3 exhibited especially high absorbency for organic solvents with special dissolving capacity, for instance tetrahydrofuran, toluene, chlorobenzene, tetrachloromethane, and dichloromethane, due to the swelling property of the porous polymer framework in these solvents. It is well-known that the swelling degree is determined by the solubility parameter (δ) of organic liquids to the polymer.[50] If the solubility parameters between the organic solvents and the polymer are close, obvious swelling of the polymer can be observed. Therefore, the influence of the

Table 3. Density and Solubility Parameter of Different Organic Solvents, Mass (M_{abs}) and Volume (V_{abs}) Absorption Capacity of the CPPs3 for the Varying Organic Solvents, And the Swell Ratio of the CPPs3 after Absorption

organic liquids	density (g/cm^3)	M_{abs} (g/g)	V_{abs} (cm^3/cm^3)	solubility parameter δ/(J$^{1/2}$cm$^{-3/2}$)	swell ratio
n-butanol	0.80	4.7	0.54	23.3	1.00
acetonitrile	0.79	5.2	0.48	24.0	1.00
cyclohexane	0.78	8.3	0.49	16.8	1.20
decalin	0.88	13.9	1.42	18.4	1.82
tetrahydrofuran	0.89	24.8	3.16	19.0	4.39
toluene	0.87	29.5	3.02	18.2	3.76
chlorobenzene	1.10	30.5	2.92	19.4	4.32
tetrachloromethane	1.60	32.0	2.12	17.6	3.17
dichloromethane	1.33	33.0	2.14	19.8	3.70

DOI: 10.1021/acsami.5b00196
ACS Appl. Mater. Interfaces 2015, 7, 6745−6753

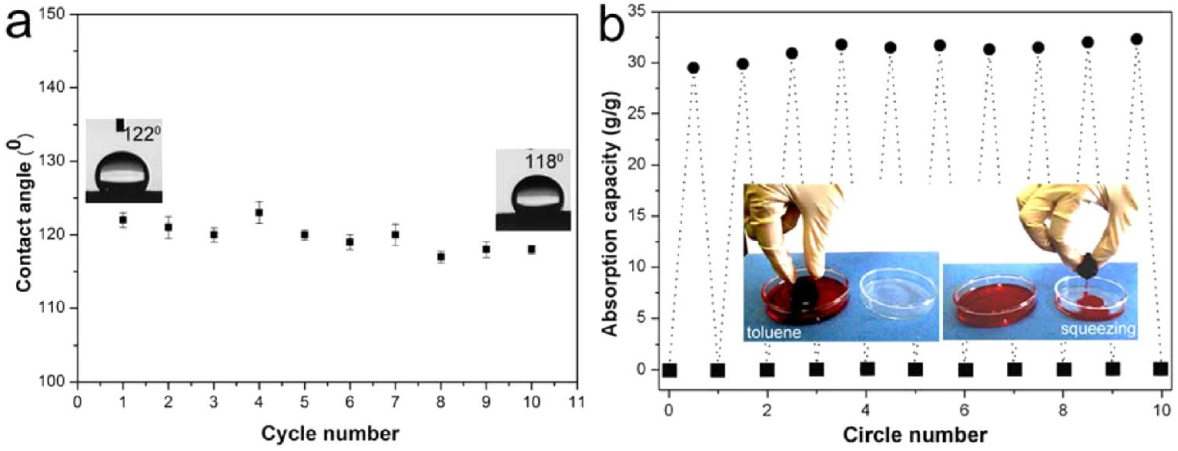

Figure 6. (a) Water contact angle of the CPPs3 as a function of the recycling number. (b, ■) Restored weight of the CPPs3 after remove of toluene, (●) weight gain after absorbing toluene during different cycles, and (insets) a simple squeezing process after absorption.

solubility parameters between the organic solvents and the polystyrene on the absorption capacity of the CPPs3 was investigated. To eliminate interference for varying densities of organic liquids, we measured volume absorption capacities to explore the role of swell ratio. When volume absorption capacities were larger than 1 cm^3/cm^3, organic solvents possess solubility parameters ranging from 17.6 to 19.8 $J^{1/2}$ $cm^{-3/2}$, which is extremely close to the solubility parameter of polystyrene (17.4−19.0 $J^{1/2}$ $cm^{-3/2}$). Moreover, the sample absorbed less than 1 cm^3/cm^3 solvents with larger (23.3 and 24 $J^{1/2}$ $cm^{-3/2}$) or smaller (16.8 $J^{1/2}$ $cm^{-3/2}$) solubility parameter showed nearly no swelling, such as n-butanol, acetonitrile, and cyclohexane. As expected, a suitable solubility parameter of organic liquids leads to the high swelling degree of the CPPs3 and, thereby, significantly increased volume absorption capacity. In addition, the absorption of crude oil had also been investigated. The result showed that the mass absorption capacity and the volume absorption capacity of the crude oil were 3.4 g/g and 0.51 cm^3/cm^3, respectively. We believe that the unsuitable solubility parameter and high viscosity of crude oil lead to the low swelling degree of the CPPs and, thereby, low absorption capacity. In a word, it offers a strategy to design high absorbent polymers for specific organic solvents via tuning composition of porous polymeric framework.

In addition, it should be noted that the CPPs transformed from rigid to sponge-like materials once the organic solvents were absorbed. This change in rigidity enables the elastically active networked structure of the material to stretch.[51] This means the CPPs oil absorbents can be recycled by manually compressing the material, as exhibited in the inset of Figure 6 and movie S2 Supporting Information. More than 70% of the organic solvents could be collected by squeezing the material (Table S1, Supporting Information). To test the recyclability of the CPPs oil absorbents, toluene as probe organic solvent was absorbed repeatedly, and the result is shown in Figure 6. The CPPs were regenerated with squeezing and drying at ambient temperature. The materials basically retained their hydrophobicity and high absorbency after 10 cycles, indicating that it is a good candidate for oil cleanup application with reduced cost.

Gas Permeability Performance of IPPs Materials. Gas permeability is another important property of porous polymeric materials. Therefore, the gas permeability coefficient of IPPs as a function of pressure curves is drawn in Figure 7. The gas

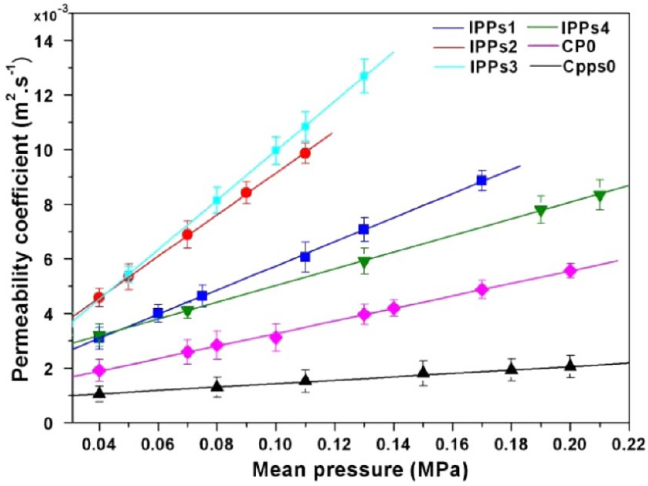

Figure 7. Permeability coefficient curve of the IPPs, CP0, and CPPs0 with varying mean pressure and gas permeability (k) determined by the slope of the fitting line.

permeability coefficient was calculated according to Darcy's law. The gas permeability, namely, viscous permeability value (denoted as k), was determined by gas permeability coefficient and mean pressure. The value of k was obtained by the slope of the individual permeability coefficient versus pressure curves and is summarized in Table 2. All of the slopes of the curve of IPPs are higher than both the conventional poly-HIPE (CP0) and CPPs0. Even IPPs2 with the least number of pore throats among the IPPs had a gas permeability of 0.78 D, which was 7 times larger than that of CPPs0, resulting from increasing pore interconnectivity. In addition, the gas permeability presents a strong dependence on the number of pore throats that bridge the neighboring pores. As the amount of surfactant increases from 2 to 5%, the gas permeability increases consistently from IPPs1 to IPPs3. However, there was a sudden drop in gas permeability of IPPs4 compared with other IPPs,due to the reduction in average pore throats size and disappearance of supermacropores.

■ CONCLUSIONS

In summary, amphiphilic carbonaceous microspheres exhibit a versatile ability to stabilize high internal phase water-in-oil Pickering emulsions. Two types of monolith high-porosity

DOI: 10.1021/acsami.5b00196
ACS Appl. Mater. Interfaces 2015, 7, 6745−6753

supermacroporous polystyrene materials with high mechanical strength had been controlled synthesized from these emulsions. The CPPs exhibit excellent abilities for oil−water separation, while the IPPs possess good gas permeability. More importantly, a new strategy was proposed tunning composition of porous framework, which may pave a new way for designing highly absorbent polymers for specific organic solvents.

■ ASSOCIATED CONTENT

Supporting Information

SEM of the carbonaceous microspheres, FTIR spectra of surface functional groups of CMs, optical microscopy images of HIPEs, SEM of porous surface of CPPs and IPPs1, and the movies that show the absorbing process and hardness change of CPPs3. This material is available free of charge via the Internet at http://pubs.acs.org.

■ AUTHOR INFORMATION

Corresponding Author

*E-mail: kbzhou@ucas.ac.cn.

Author Contributions

All authors have given approval to the final version of the manuscript.

Funding

This work was supported by the National Natural Science Foundation of China (91127018, U1162113).

Notes

The authors declare no competing financial interest.

■ REFERENCES

(1) Gandara, F.; Furukawa, H.; Lee, S.; Yaghi, O. M. High Methane Storage Capacity in Aluminum Metal−Organic Frameworks. *J. Am. Chem. .Soc.* **2014**, *136*, 5271−5274.

(2) Furukawa, H.; Yaghi, O. M. Storage of Hydrogen, Methane, and Carbon Dioxide in Highly Porous Covalent Organic Frameworks for Clean Energy Applications. *J. Am. Chem. Soc.* **2009**, *131*, 8875−8883.

(3) Furukawa, H.; Gandara, F.; Zhang, Y. B.; Jiang, J.; Queen, W. L.; Hudson, M. R.; Yaghi, O. M. Water Adsorption in Porous Metal−Organic Frameworks and Related Materials. *J. Am. Chem. Soc.* **2014**, *136*, 4369−4381.

(4) Wang, B.; Liang, W. X.; Guo, Z. J.; Liu, W. M. Biomimetic Super-Lyophobic and Super-Lyophilic Materials Applied for Oil/Water Separation: A New Strategy beyond Nature. *Chem. Soc. Rev.* **2015**, *44*, 336−361.

(5) Zhang, Y. J.; Wang, S. P.; Mohammad, E.; Motamedi, M.; Kotov, N. A. Inverted-Colloidal-Crystal Hydrogel Matrices as Three-Dimensional Cell Scaffolds. *Adv. Funct. Mater.* **2005**, *15*, 725−731.

(6) Hu, Y.; Gu, X. Y.; Yu, Y.; Jian, H.; Huang, J.; Hu, M.; Chen, W. K.; Tong, Z.; Wang, C. Y. Facile Fabrication of Poly(L-lactic acid)-Grafted Hydroxyapatite/Poly(lactic-co-glycolic Acid) Scaffolds by Pickering High Internal Phase Emulsion Templates. *ACS Appl. Mater. Interfaces* **2014**, *6*, 17166−17175.

(7) Pierre, S. J.; Thies, J. C.; Dureault, A.; Cameron, N. R.; Hest, J. C. M. v.; Carette, N.; Michon, T.; Weberskirch, R. Covalent Enzyme Immobilization onto Photopolymerized Highly Porous Monoliths. *Adv. Mater.* **2006**, *18*, 1822−1826.

(8) Zhang, Y. G.; Zhao, L.; Patra, P. K.; Ying, J. Y. Synthesis and Catalytic Applications of Mesoporous Polymer Colloids in Olefin Hydrosilylation. *Adv. Synth. Catal.* **2008**, *350*, 662−666.

(9) Chan-Thaw, C. E.; Villa, A.; Katekomol, P.; Su, D.; Thomas, A.; Prati, L. Covalent Triazine Framework as Catalytic Support for Liquid Phase Reaction. *Nano Lett.* **2010**, *10*, 537−541.

(10) Kovacic, S.; Anzlovar, A.; Erjavec, B.; Kapun, G.; Matsko, N. B.; Zigon, M.; Zagar, E.; Pintar, A.; Slugovc, C. Macroporous ZnO Foams by High Internal Phase Emulsion Technique: Synthesis and Catalytic Activity. *ACS Appl. Mater. Interfaces* **2014**, *6*, 19075−19081.

(11) Wang, Y.; He, C. H.; Xing, W. H.; Li, F. B.; Tong, L.; Chen, Z. Q.; Liao, X. Z.; Steinhart, M. Nanoporous Metal Membranes with Bicontinuous Morphology from Recyclable Block-Copolymer Templates. *Adv. Mater.* **2010**, *22*, 2068−2072.

(12) Cho, H.; Park, H.; Russell, T. P.; Park, S. Precise Placements of Metal Nanoparticles from Reversible Block Copolymer Nanostructures. *J. Mater. Chem.* **2010**, *20*, 5047−5051.

(13) Zhang, Y. G.; Zhao, L.; Patra, P. K.; Ying, J. Y. Synthesis and Catalytic Applications of Mesoporous Polymer Colloids in Olefin Hydrosilylation. *Adv. Synth. Catal.* **2008**, *350*, 662−666.

(14) Thomas, A.; Goettmann, F.; Antonietti, M. Hard Templates for Soft Materials: Creating Nanostructured Organic Materials. *Chem. Mater.* **2008**, *20*, 738−755.

(15) Wang, Y.; Li, F. B. An Emerging Pore-Making Strategy: Confined Swelling-Induced Pore Generation in Block Copolymer Materials. *Adv. Mater.* **2011**, *23*, 2134−2148.

(16) Olson, D. A.; Chen, L.; Hillmyer, M. A. Templating Nanoporous Polymers with Ordered Block Copolymers. *Chem. Mater.* **2008**, *20*, 869−890.

(17) Li, W. W.; Yoon, J. A.; Matyjaszewski, K. Dual-Reactive Surfactant Used for Synthesis of Functional Nanocapsules in Miniemulsion. *J. Am. Chem. Soc.* **2010**, *132*, 7823−7825.

(18) Kimmins, S. D.; Cameron, N. R. Functional Porous Polymers by Emulsion Templating: Recent Advances. *Adv. Funct. Mater.* **2011**, *21*, 211−225.

(19) Wu, D. C.; Xu, F.; Sun, B.; Fu, R. W.; He, H. K.; Matyjaszewski, K. Design and Preparation of Porous Polymers. *Chem. Rev.* **2012**, *112*, 3959−4015.

(20) Ikem, V. O.; Menner, A.; Bismarck, A. High Internal Phase Emulsions Stabilized Solely by Functionalized Silica Particles. *Angew. Chem., Int. Ed.* **2008**, *47*, 8277−8279.

(21) Ikem, V. O.; Menner, A.; Bismarck, A. High-Porosity Macroporous Polymers Sythesized from Titania-Particle-Stabilized Medium and High Internal Phase Emulsions. *Langmuir* **2010**, *26*, 8836−8841.

(22) Cai, D. Y.; Thijssen, J. H. T.; Clegg, P. S. Making Non-aqueous High Internal Phase Pickering Emulsions: Influence of Added Polymer and Selective Drying. *ACS Appl. Mater. Interfaces* **2014**, *6*, 9214−9219.

(23) Ikem, V. O.; Menner, A.; Horozov, T. S.; Bismarck, A. Highly Permeable Macroporous Polymers Synthesized from Pickering Medium and High Internal Phase Emulsion Templates. *Adv. Mater.* **2010**, *22*, 3588−3592.

(24) Haibach, K.; Menner, A.; Powell, R.; Bismarck, A. Tailoring Mechanical Properties of Highly Porous Polymer Foams: Silica Particle Reinforced Polymer Foams via Emulsion Templating. *Polymer* **2006**, *47*, 4513−4519.

(25) Silverstein, M. S. PolyHIPEs: Recent Advances in Emulsion-Templated Porous Polymers. *Prog. Polym. Sci.* **2014**, *39*, 199−234.

(26) Sadeghpour, A.; Pirolt, F.; Glatter, O. Submicrometer-Sized Pickering Emulsions Stabilized by Silica Nanoparticles with Adsorbed Oleic Acid. *Langmuir* **2013**, *29*, 6004−6012.

(27) Vílchez, A.; Rodríguez-Abreu, C.; Esquena, J.; Menner, A.; Bismarck, A. Macroporous Polymers Obtained in Highly Concentrated Emulsions. *Langmuir* **2011**, *27*, 13342−13352.

(28) Zhang, S. M.; Chen, J. D. PMMA Based Foams Made via Surfactant-Free High Internal Phase Emulsion Templates. *Chem. Commun.* **2009**, *16*, 2217−2219.

(29) Ni, D. Z.; Wang, L.; Sun, Y. H.; Guan, Z. R.; Yang, S.; Zhou, K. B. Amphiphilic Hollow Carbonaceous Microspheres with Permeable Shells. *Angew. Chem. Int. .Ed.* **2010**, *49*, 4223−4227.

(30) Wang, L.; Ni, D. Z.; Yang, D.; Zhou, K. B.; Yang, S. Single-Hole Carbonaceous Microcapsules. *Chem. Lett.* **2010**, *39*, 451−453.

(31) Tan, H. Y.; Zhang, P.; Wang, L.; Yang, D.; Zhou, K. B. Multifunctional Amphiphilic Carbonaceous Microcapsules Catalyze Water/Oil Biphasic Reactions. *Chem. Commun.* **2011**, *47*, 11903−11905.

DOI: 10.1021/acsami.5b00196
ACS Appl. Mater. Interfaces 2015, 7, 6745−6753

(32) Zhu, Z. B.; Tan, H. Y.; Wang, J.; Yu, S. Z.; Zhou, K. B. Hydrodeoxygenation of Vanillin as A Bio-Oil Model over Carbonaceous Microspheres-Supported Pd Catalysts in the Aqueous Phase and Pickering Emulsions. *Green Chem.* **2014**, *16*, 2636−2643.
(33) Akhavan, B.; Jarvis, K.; Majewski, P. Hydrophobic Plasma Polymer Coated Silica Particles for Petroleum Hydrocarbon Removal. *ACS Appl. Mater. Interfaces* **2013**, *5* (17), 8563−8571.
(34) Manley, S. S.; Graeber, N.; Grof, Z.; Menner, A.; Hewitt, G. F.; Stepanek, F.; Bismarck, A. New Insights into The Relationship Between Internal Phase Level of Emulsion Templates and Gas−Liquid Permeability of Interconnected Macroporous Polymers. *Soft Matter.* **2009**, *5*, 4780−4787.
(35) Giermanska-Kahn, J.; Laine, V.; Arditty, S.; Schmitt, V.; Leal-Calderon, F. Particle-Stabilized Emulsions Comprised of Solid Droplets. *Langmuir* **2005**, *21*, 4316−4323.
(36) Destribats, M.; Faure, B.; Birot, M.; Babot, O.; Schmitt, V.; Backov, R. Tailored Silica Macrocellular Foams: Combining Limited Coalescence-Based Pickering Emulsion and Sol-Gel Process. *Adv. Funct. Mater.* **2012**, *22*, 2642−2654.
(37) Lau, T. H. M.; Wong, L. L. C.; Lee, K. Y.; Bismarck, A. Tailored for Simplicity: Creating High Porosity, High Performance Bio-Based Macroporous Polymers from Foam Templates. *Green Chem.* **2014**, *16*, 1931−1940.
(38) Ling, L.; Wong, C.; Ikem, V. O.; Menner, A.; Bismarck, A. Macroporous Polymers with Hierarchical Pore Structure from Emulsion Templates Stabilised by Both Particles and Surfactants. *Macromol. Rapid Commun.* **2011**, *32*, 1563−1568.
(39) Ho, T. T. T.; Zimmermann, T.; Ohr, S.; Caseri, W. R. Composites of Cationic Nanofibrillated Cellulose and Layered Silicates: Water Vapor Barrier and Mechanical Properties. *ACS Appl. Mater. Interfaces* **2012**, *4*, 4832−4840.
(40) Ku, H.; Wang, H.; Pattarachaiyakoop, N.; Trada, M. A Review on the Tensile Properties of Natural Fiber Reinforced Polymer Composites. *Composites, Part B* **2011**, *42*, 856−873.
(41) Gersappe, D. Molecular Mechanisms of Failure in Polymer Nanocomposites. *Phys. Rev. Lett.* **2002**, *89*, 058301−058304.
(42) Riggleman, R. A.; Toepperwein, G.; Papakonstantopoulos, G. J.; Barrat, J. L.; de Pablo, J. J. Entanglement Network in Nanoparticle Reinforced Polymers. *J. Chem. Phys.* **2009**, *130*, 244903−244906.
(43) Gao, Y.; Qiao, Y.; Yang, S. Fabrication of PAN-PHCS Adsorptive UF Membranes with Enhanced Performance for Dichlorophenol Removal from Water. *J. Appl. Polym. Sci.* **2014**, *131*, 40837−40845.
(44) Zhang, Y. L.; Wei, S.; Liu, F. J.; Du, Y. C.; Liu, S.; Ji, Y. Y.; Yokoib, T.; Tatsumib, T.; Xiao, F. S. Superhydrophobic Nanoporous Polymers as Efficient Adsorbents for Organic Compounds. *Nano Today* **2009**, *4*, 135−142.
(45) Choi, S. J.; Kwon, T. H.; Im, H.; Moon, D.-I.; Baek, D. J.; Seol, M.-L.; Duarte, J. P.; Choi, Y.-K. A Polydimethylsiloxane (PDMS) Sponge for the Selective Absorption of Oil from Water. *ACS Appl. Mater. Interfaces* **2011**, *3*, 4552−4556.
(46) Li, A.; Sun, H. X.; Tan, D. Z.; Fan, W. J.; Wen, S. H.; Qing, X. J.; Li, G. X.; Li, S. Y.; Deng, W. Q. Superhydrophobic Conjugated Microporous Polymers for Separation and Adsorption. *Energy Environ. Sci.* **2011**, *4*, 2062−2065.
(47) Zhou, X. Y.; Zhang, Z. Z.; Xu, X. H.; Men, X. H.; Zhu, X. T. Facile Fabrication of Superhydrophobic Sponge with Selective Absorption and Collection of Oil from Water. *Ind. Eng. Chem. Res.* **2013**, *52*, 9411−9416.
(48) Zhu, Q.; Chu, Y.; Wang, Z. K.; Chen, N.; Li, L.; Liu, F. T.; Pan, Q. M. Robust Superhydrophobic Polyurethane Sponge as A Highly Reusable Oil-Absorption Material. *J. Mater. Chem.A* **2013**, *1*, 5386−5396.
(49) Das, D.; Gaur, V.; Verma, N. Removal of Volatile Organic Compound by Activated Carbon Fiber. *Carbon* **2004**, *42*, 2949−2962.
(50) Zhang, A. J.; Chen, M. J.; Du, C.; Guo, H. Z.; Bai, H.; Li, L. Poly(dimethylsiloxane) Oil Absorbent with a Three-Dimensionally Interconnected Porous Structure and Swellable Skeleton. *ACS Appl. Mater. Interfaces* **2013**, *5*, 10201−10206.
(51) Flory, P. J.; Rehner, J. Statistical Mechanics of Cross-Linked Polymer Networks II. Swelling. *J. Chem. Phys.* **1943**, *11*, 521−526.

DOI: 10.1021/acsami.5b00196
ACS Appl. Mater. Interfaces 2015, 7, 6745−6753